Murine DNA (Cytosine-5-)-methyltransferase: Steady-State and Substrate Trapping Analyses of the Kinetic Mechanism

James Flynn and Norbert Reich*

Department of Chemistry and Program in Biochemistry and Molecular Biology, University of California, Santa Barbara, California 93106

Received May 7, 1998; Revised Manuscript Received August 19, 1998

ABSTRACT: DNA (cytosine-5-)-methyltransferase is essential for viable mammalian development and has a central function in the determination and maintenance of epigenetic methylation patterns. Steady-state and substrate trapping studies were performed to better understand how the enzyme functions. The catalytic efficiency was dependent on substrate DNA length. A 14-fold increase in K_m^{DNA} was observed as the length decreased from 5000 to 100 base pairs and k_{cat} decreased by a third. Steady-state analyses were used to identify the order of substrate addition onto the enzyme and the order of product release. Double-reciprocal patterns of velocity versus substrate concentration intersected far from the origin and were nearly parallel. The kinetic mechanism does not appear to change when the DNA substrate is either 6250 or 100 base pairs in length. Isotope trapping studies showed that the initial enzyme−AdoMet complex was not catalytically competent; however, the initial enzyme−poly(dI·dC−dI·dC) complex was observed to be competent for catalysis. Product inhibition studies also support a sequential ordered bi-bi kinetic mechanism in which DNA binds to the enzyme first, followed by *S*-adenosyl-L-methionine, and then the products *S*-adenosyl-L-homocysteine and methylated DNA are released. The proposed mechanism is similar to the mechanism proposed for M.*Hha*I, a bacterial DNA (cytosine-5-)-methyltransferase. Evidence for an enzyme−DNA−DNA ternary complex is also presented.

In eukaryotic organisms, DNA methylation is catalyzed by an *S*-adenosyl-L-methionine- (AdoMet-)[1] dependent DNA (cytosine-5-)-methyltransferase (DCMTase, EC 2.1.1.37). Methyl group transfer to the cytosine 5-position occurs predominantly within the cytosyl-guanosyl (CpG) context (*1*), and the genomic distribution of 5-methylcytosine (5-^{m}C) dynamically changes throughout ontogeny (*2*, *3*). DCMTase is involved in mammalian development by way of an undefined process that can lead to gene regulation (reviewed in ref *4*). Proper DCMTase function is essential for viable development and for normal cellular activity (*5*). Also, errors in the proper maintenance of genomic methylation occur in aging and carcinogenesis (*6*, *7*).

Eukaryotic DCMTase cDNAs have been cloned and sequenced; five are from animal sources (mouse, *8*; human, *9*; chicken, *10*; frog, *11*; and sea urchin, *12*). DCMTases are composed of a large amino-terminal domain and a smaller carboxy-terminal domain that contains many of the major motifs found in prokaryotic DNA (cytosine-5-)-methyltransferases (*13*). The amino-terminal domain has been implicated in nuclear localization to DNA replication foci during S-phase (*14*), metal binding by zinc finger domains, and DNA binding (*15*, *16*). The murine DCMTase is a large 183 kDa protein that contains a serine residue that is phosphorylated (*17*). The enzyme presumably interacts with many cellular factors in a complex signaling pathway that regulates DNA methylation levels.

Enzymes that catalyze one-carbon additions to the C^5 position of pyrimidines define a class of enzymes that perform similar chemistry (*18*). The bacterial DNA (cytosine-5-)-methyltransferase, M.*Hha*I (38 kDa), modifies the internal cytosine in G$\underline{C}$GC and has a rapid equilibrium ordered bi-bi kinetic mechanism in which DNA binds the enzyme first (*19*). Catalysis involves nucleophilic attack by the thiol of an active-site cysteine at the C^6 position of cytosine, which in the absence of the cofactor leads to exchange of the C^5 hydrogen. A M.*Hha*I−DNA cocrystal structure suggests that a catalytic intermediate exists that involves the translocation of the target cytosine to an extrahelical position (*20*). Methyl transfer from AdoMet is followed by β-elimination to regenerate the free enzyme by releasing *S*-adenosyl-L-homocysteine (AdoHcy) followed by methylated DNA (*19*, *21*).

The involvement of DNA (cytosine-5-)-methyltransferases in mammalian tumorigenesis (*22*, *23*) and the need for therapeutic alternatives to treat human cancers (*6*, *7*) capitalize on the importance of a more complete enzymological description of these enzymes. Understanding the catalytic mechanism is a first step in precisely defining how DCMTase is regulated by cellular factors (*24*, *25*) and can be used to evaluate the functional differences of alternatively expressed DNA (cytosine-5-)-methyltransferase enzymes (*17*, *26*, *27*). We have been using a highly homogeneous, unproteolyzed

† This work was supported by NIH Grant GM 56289.

* To whom correspondence should be addressed.

[1] Abbreviations: 5-^{m}C, 5-methylcytosine; AdoHcy, *S*-adenosyl-L-homocysteine; AdoMet, *S*-adenosyl-L-methionine; DCMTase, DNA (cytosine-5-)-methyltransferase; MEL, Friend murine erythroleukemia cells; M.*Hha*I, DNA (cytosine-5-)-methyltransferase from *Haemophilus haemolyticus;* M.*Sss*I, DNA (cytosine-5-)-methyltransferase from *Spiroplasma*; pdIdC, poly(dI·dC−dI·dC).

10.1021/bi9810609 CCC: $15.00
Published on Web 10/10/1998

preparation of DCMTase from mouse erythroleukemia cells (MEL; *28*) to study DNA methylation. We determined that the enhanced enzyme activity often observed with hemimethylated DNA compared to unmethylated substrates derives from a 10-fold higher catalytic rate constant, $k_{methylation}$ (*29*). The initial DNA binding event was sequence-dependent and K_m^{DNA} for small, single CpG-containing DNA is similar to K_D^{DNA} (*30*). In this report, we further characterize the interactions of DCMTase with the substrates, poly(dI·dC−dI·dC) and AdoMet, and the products, methylated poly(dI·d^{m}C−dI·d^{m}C) and AdoHcy.

EXPERIMENTAL PROCEDURES

Materials. *S*-Adenosyl-L-[*methyl*-^{3}H]methionine (75 Ci/mmol, 1 mCi/mL, 1 Ci = 37 GBq) was purchased from Amersham Corp. Unlabeled AdoMet (Sigma Chemical Co.) was further purified as described (*29*). Routinely, 125 μM AdoMet stocks were prepared at a specific activity of 5.8×10^3 cpm/pmol. Two lots of poly(dI·dC−dI·dC) were purchased from Pharmacia Biotech, Inc., with an average length of 6250 and 5000 base pairs. DE81 filters were purchased from Whatman, Inc. Other standard chemicals and reagents were purchased from Sigma Chemical Co. or Fisher Scientific.

DNA (cytosine-5-)-methyltransferase was purified from mouse erythroleukemia cells as described (*28*). Two separate preparations, with concentrations of 380 and 260 nM, were confirmed to have equivalent activities with the substrates studied.

Steady-State Kinetic Assays. The DNA substrate used was poly(dI·dC−dI·dC). This substrate contains tandem methylation sites in which guanine has been replaced by inosine. Methylation is catalyzed at a higher rate with this substrate than with other DNA (*29*, *31*). Poly(dI·dC−dI·dC) provides a uniform sequence and limits the potential complexities found with large cloned sequences that contain many randomly situated CpG dinucleotides, each having different flanking sequence contributions to binding and catalysis (*29*, *30*).

Duplicate 25 μL reaction volumes contained DCMTase and AdoMet in MR buffer (100 mM Tris-HCl, pH 8.0, 10 mM EDTA, 200 μg/mL BSA, and 10 mM DTT). After preincubation at room temperature for up to 10 min, reactions were initiated by the addition of poly(dI·dC−dI·dC) and, if indicated, reaction products. The substrate and product concentrations were varied as indicated in the figures. In several experiments it was found that initiating a reaction containing DNA with AdoMet yielded similar results to the conditions routinely used. After 60 min at 37 °C, the reaction was stopped by transferring 20 μL onto DE 81 filter paper. Filters were washed (200 mL) in the following order: three times with 50 mM K_2HPO_4 and one time each with 80% ethanol, 95% ethanol, and diethyl ether. Dried filters were placed in 3 mL of LiquiScint (National Diagnostics) and disintegrations were counted on a Beckman LS1701 liquid scintillation counter. The radioactivity above the background, from assays without added poly(dI·dC−dI·dC), was converted to initial velocities and expressed as picomoles of methyl groups transferred to poly(dI·dC−dI·dC) per hour and plotted in double-reciprocal form.

Fragmentation of Poly(dI·dC−dI·dC). Sonication was used to break a 5000 base pair average length poly(dI·dC−dI·dC) to lengths of approximately 2000, 1400, 600, 500, and 100 base pairs with a Branson Sonifier 450 with a microbore tip. Lengths were estimated by agarose gel electrophoresis using DNA size standards.

Preparation of Poly(dI·d^{m}C−dI·d^{m}C). Poly(dI·dC−dI·dC) was methylated to completion with M.*Sss*I (New England Biolabs). The methylation reaction was optimized and the apparent K_m^{DNA} was determined to be 0.40 nM for M.*Sss*I using 6250 base pair poly(dI·dC−dI·dC). For reaction efficiency and sufficient yields, a 500 μL reaction contained 1.0 nM poly(dI·dC−dI·dC). AdoMet was added to 100 μM to provide an excess level of methyl groups to complete the reaction. Three 20-unit aliquots of M.*Sss*I were added every 10 h in MR buffer. After the DNA was cleaned by standard organic extraction methods, it was resuspended to 10 nM in TE (10 mM Tris, pH 8.0, and 1 mM EDTA) and subjected to the methylation reaction using M.*Sss*I and radiolabeled AdoMet. Background, 230 cpm, was detected with this preparation at 0.80 nM and a similar control experiment with 0.80 nM unmethylated poly(dI·dC−dI·dC) generated 37 000 cpm. The methylated DNA, poly(dI·d^{m}C−dI·d^{m}C), was resistant to digestion by *Hha*I endonuclease and the control DNA was digested to small fragments, as determined by agarose gel electrophoresis.

Isotope Partitioning Analysis. A pulse−chase approach was used to determine the catalytic competency of the DCMTase−AdoMet complex. The complex was formed at 37 °C with 20 nM DCMTase and tritiated AdoMet at a concentration of 10 μM. The reaction was initiated by adding a mixture of 400 pM poly(dI·dC−dI·dC) and 100 μM unlabeled AdoMet. After a 1 h incubation at 37 °C, the reactions were treated as stated above.

Molecular Partitioning Analysis. A substrate trapping approach was used to determine the catalytic competency of the DCMTase−DNA complex. Two different sizes of substrate DNA, 1400 and 600 base pair poly(dI·dC−dI·dC), were used to distinguish if the initial complex proceeded in the forward direction or dissociated before DCMTase performed chemistry. The complex was formed at 37 °C for 1.5 min with 5 nM DCMTase and the 1400 base pair poly(dI·dC−dI·dC) at 0.20 nM, and then a mixture containing 2.0 μM tritiated AdoMet (neat stock concentration, 13 μM) plus an excess of the molecular competitor, 600 base pair poly(dI·dC−dI·dC) at 5.0 nM was added to initiate catalysis. Aliquots were removed at 1.5, 3, and 9 min followed by centrifugation through a P-6 spin column (Bio-Rad) to trap unincorporated label. DNA samples were separated on a 6% polyacrylamide, 8 M urea gel run at 400 V for 4.5 h. Standard methods of fluorography were used with LiquiScint (National Diagnostics) as the fluor. The dried gel was exposed to Fuji XAR film for 3 months at −70 °C.

Data Analysis. The Michaelis−Menten equation was used for studies into DNA length contributions to catalysis using KaleidaGraph 2.1.2 (Synergy Software). For mechanistic determinations the nomenclature used is that of Cleland (*32*, *33*) and data were analyzed by regression analysis of the appropriate initial velocity equation, listed below, using the Cleland programs (*34*). The algorithms perform a nonlinear least-squares fit to the entire data set. Mechanistic determinations were made by comparison of the σ values associated with the fit to each equation. The standard errors

associated with fitted parameters and graphical analysis of the experimental data scattered around the calculated best-fit lines were also considered in making an assignment.

hyperbola:

$$v = \frac{VA}{K_{mA} + A} \quad (1)$$

sequential mechanism:

$$v = \frac{VAB}{K_{ia}K_{mB} + K_{mA}B + K_{mB}A + AB} \quad (2)$$

ping-pong mechanism:

$$v = \frac{VAB}{K_{mA}B + K_{mB}A + AB} \quad (3)$$

competitive inhibition:

$$v = \frac{VA}{K_{mA}(1 + I/K_{is}) + A} \quad (4)$$

noncompetitive inhibition:

$$v = \frac{VA}{K_{mA}(1 + I/K_{is}) + A(1 + I/K_{ii})} \quad (5)$$

uncompetitive inhibition:

$$v = \frac{VA}{K_{mA} + A(1 + I/K_{ii})} \quad (6)$$

The parameters are as follows: v, initial velocity; V, maximum velocity; A, concentration of substrate A; B, concentration of substrate B; K_m, Michaelis constant; K_{is} and K_{ii}, slope and intercept inhibition constants, respectively; I, inhibitor concentration.

RESULTS AND DISCUSSION

The need for a functional and structural understanding of the rapidly expanding group of mammalian DNA cytosine methyltransferases is made ever more pressing, following reports implicating DNA methylation in chromatin restructuring and in the early stages of tumorigenesis through both tumor suppressor genes and DNA repair processes. The selection of a suitable substrate for the investigation of a DNA modifying enzyme is particularly complex; are single or multisite substrates preferred, short synthetic or longer fragments harboring biologically relevant sequences, linear or supercoiled molecules? Our choice of poly(dI·dC−dI·dC) for use in the kinetic mechanism studies was based in part on our prior demonstration that the mammalian enzyme shows significantly better activity with this substrate than others. Initial velocity studies with poly(dI·dC−dI·dC) result in very low levels of product formation, thereby circumventing the potentially complicating issue of how adjacent methyl groups alter the kinetics of methylation.

DNA Length Contributions to Catalytic Efficiency. We initially sought to determine which length of poly(dI·dC−dI·dC) showed the highest catalytic efficiency with the enzyme. Initial velocity profiles were obtained for poly(dI·dC−dI·dC) lengths of approximately 5000, 2000, 500, and 100 base pairs (Figure 1). The kinetic terms are compared in Table 1. A 14-fold increase in K_m^{DNA} was observed as the length decreased from 5000 to 100 base pairs and k_{cat} decreased by a third. The apparent first-order rate constant at low substrate concentrations, k_{cat}/K_m^{DNA}, is a measure of catalytic efficiency, and the hyperbolic trend (Figure 2) suggests a half-maximal DNA length of 1200 base pairs and that lengths greater than 2000 base pairs provide little more to catalytic efficiency. In contrast, DNA lengths of 500 base pairs and smaller show a very sharp decrease in efficiency.

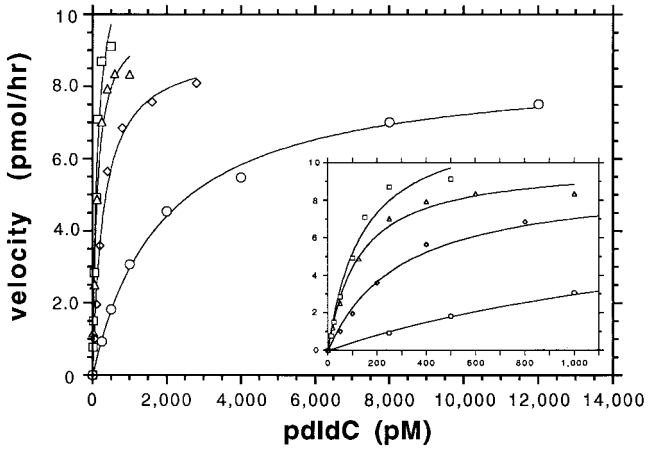

FIGURE 1: Initial velocity plots of different poly(dI·dC−dI·dC) lengths. Reactions contained 20 nM DCMTase and 10 μM AdoMet in 100 mM Tris, pH 8.0, 10 mM EDTA, 10 mM DTT, and 200 μg/mL BSA. Incubations were at 37 °C for 60 min. The poly(dI·dC−dI·dC) lengths were (○) 100 base pairs: (◇) 500 base pairs; (△) 2000 base pairs; and (□) 5000 base pairs. Data were fitted to the Michaelis−Menten equation and the constants derived from eq 1 are summarized in Table 1. The inset shows the quality of the data close to the *y*-axis.

Table 1: Poly(dI·dC−dI·dC) Length and Catalytic Efficiency[a]

length	V_{max} (pmol h^{-1})	k_{cat} (h^{-1})	K_m (pM)	k_{cat}/K_m (M^{-1} s^{-1} × 10^7)
5000	12.5 ± 1.1	31.2	140 ± 30	6.2
2000	9.95 ± 0.39	24.9	125 ± 17	5.5
500	9.12 ± 0.29	22.8	300 ± 30	2.1
100	8.60 ± 0.21	21.5	1890 ± 150	0.31

[a] Apparent constants were determined from initial velocity analysis using the Michaelis−Menten equation.

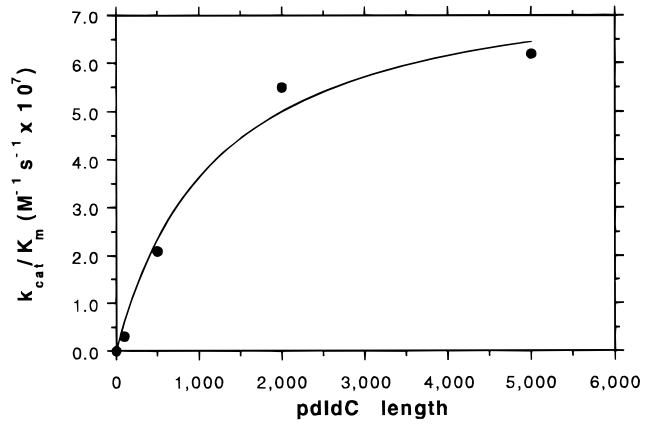

FIGURE 2: DCMTase efficiency as a function of poly(dI·dC−dI·dC) length. The apparent constants were derived from Figure 1 and are shown in Table 1. The data were fitted well by an isotherm that yielded a half-maximal length of 1200 base pairs and a maximal k_{cat}/K_m value of 8.0 × 10^7 M^{-1} s^{-1}.

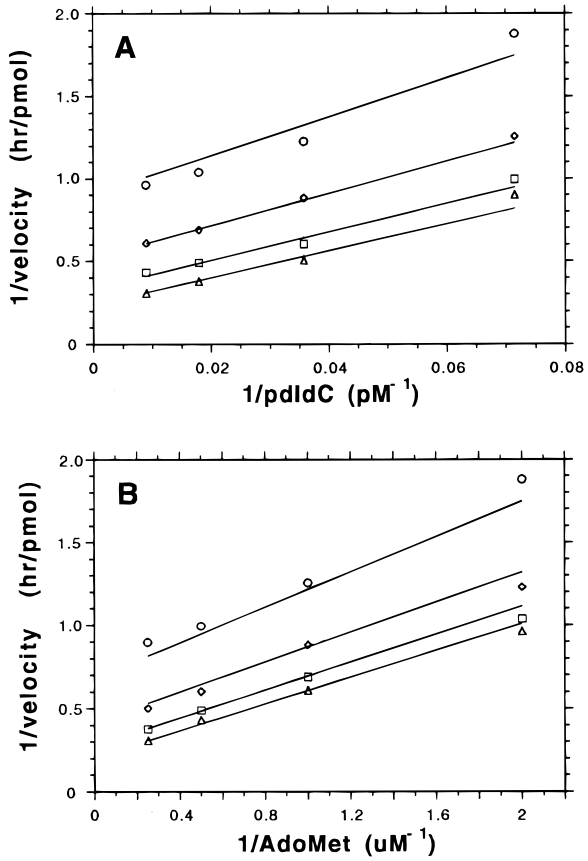

FIGURE 3: Double-reciprocal plots of velocity vs substrate concentration. Reactions contained 20 nM DCMTase in 100 mM Tris, pH 8.0, 10 mM EDTA, 10 mM DTT, and 200 μg/mL BSA. Incubations were at 37 °C for 60 min. (Panel A) Poly(dI·dC−dI·dC) is varied and lines represent a constant AdoMet concentration: (△) 4.0 μM; (□) 2.0 μM; (◇) 1.0 μM; and (○) 0.50 μM. (Panel B) AdoMet is varied and lines represent a constant poly(dI·dC−dI·dC) concentration: (△) 112 pM; (□) 56 pM; (◇) 28 pM; and (○) 14 pM. Experimental data are shown scattered around lines derived from the fit of eq 2 for a sequential mechanism.

Similar increases in catalytic efficiency with larger DNA lengths have been demonstrated for various DNA modifying enzymes, including DNA methyltransferases. Although not demonstrated here, this dependency has uniformly been shown to involve a facilitated diffusion process in which a protein initially binds the DNA, rapidly translocates along the DNA, and binds tightly at a cognate site. The apparent first-order rate constant, k_{cat}/K_m^{DNA}, was determined to have a maximum efficiency of 8.0×10^7 M^{-1} s^{-1} (Figure 2) and is within an order of magnitude of the diffusion-controlled limit for bimolecular interactions. This correlates very well with the k_{cat}/K_m^{DNA} reported for M.*Hha*I, 6.7×10^7 M^{-1} s^{-1} (*19*). Previous work on facilitated diffusion with the bacterial DNA adenine-N^6 methyltransferase, M.*Eco*RI, indicates that the major effect of DNA length was to increase the second-order rate constant k_{on} (*35*, *36*). More studies are required to decipher which rate constants are most affected with the mammalian enzyme.

Initial Velocity Studies with Poly(dI·dC−dI·dC) and AdoMet. Double-reciprocal plots of initial velocity versus substrate concentration are shown in Figure 3, using a 6250 base pair poly(dI·dC−dI·dC). The transformed data were best fitted by lines intersecting far left of the *y*-axis using a nonlinear regression of eq 2, a standard equation for analyzing sequential steady-state mechanisms. The true Michaelis constants derived were $K_m^{pdIdC} = 36 \pm 5$ pM and $K_m^{AdoMet} = 1.4 \pm 0.2$ μM. The values determined for the dissociation constants K_i^{pdIdC} and K_i^{AdoMet} were both 10-fold smaller than the corresponding K_m values. A similar pattern of lines on double-reciprocal plots was observed when a 100 base pair poly(dI·dC−dI·dC) was used, suggesting that the length of the poly(dI·dC−dI·dC) substrate did not have an effect on the steady-state mechanism (data not shown).

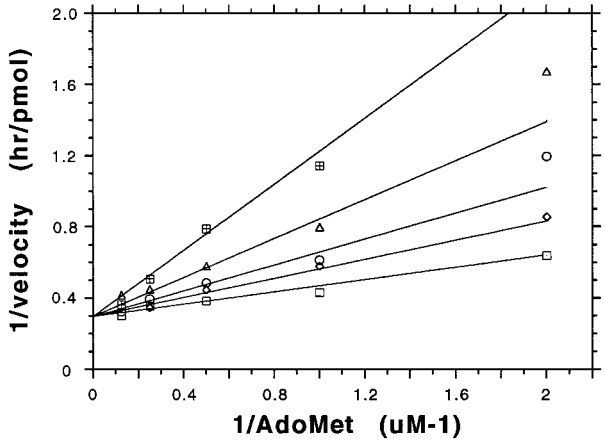

FIGURE 4: Double-reciprocal plot of AdoHcy product inhibition with varying AdoMet concentrations. Reactions contained 20 nM DCMTase and 40 pM poly(dI·dC−dI·dC) in 100 mM Tris, pH 8.0, 10 mM EDTA, 10 mM DTT, and 200 μg/mL BSA. The AdoMet concentrations were 0.50, 1.0, 2.0, 4.0, and 8.0 μM. The AdoHcy concentrations were (□) 0; (◇) 0.75 μM; (○) 1.5 μM; (△) 3.0 μM; and (notched square) 6.0 μM. Incubations were at 37 °C for 60 min. Experimental data are shown scattered around lines derived from a fit to eq 4 for competitive inhibition.

The intersecting patterns rule out a nonsequential mechanism and implicate a sequential order of substrate addition in which both DNA and AdoMet add to the enzyme surface before products are released. The nearly parallel lines can be indicative of an ordered bi-bi mechanism where $K_{ia} \ll K_{mA}$, a rapid equilibrium random mechanism where the binding of one substrate strongly inhibits the binding of the other substrate, or a nonrapid equilibrium random bi-bi mechanism where the rate constants for release of A and B are lower than k_{cat}.

Product Inhibition. Product inhibition studies were pursued to further examine the steady-state kinetic mechanism (*37*, *38*). Product inhibition is classically examined by the slopes and *y*-axis intercepts from families of double-reciprocal plots (*33*). One substrate is held constant while both the product and the substrate being studied are varied in a concentration range around its Michaelis constant. Inhibition profiles are characterized as either competitive, noncompetitive, or uncompetitive. The inhibition constants K_{ii} and K_{is} are derived from analysis of the intercept and slope effects in secondary replots, respectively, and can be either linear in a simple system or parabolic in a more complex one. The addition of products can change the normal reaction sequence by populating certain forms of the enzyme not present when products are withheld. The results from our studies are summarized in Table 2 and are described in detail below.

Product Inhibition with AdoHcy. The DCMTase reaction product AdoHcy was a linear competitive inhibitor of AdoMet (Figure 4). A nonrapid equilibrium random bi-bi

Table 2: Product Inhibition of Murine DNA (Cytosine-5-)-methyltransferase[a]

product	varied substrate	fixed substrate	type of inhibition	inhibition constant[b]
poly(dI·d^{m}C−dI·d^{m}C)	poly(dI·dC−dI·dC)	AdoMet	NC	nd[c]
poly(dI·d^{m}C−dI·d^{m}C)	AdoMet	poly(dI·dC−dI·dC)	NC	K_{is} 5.3 ± 2.1 pM K_{ii} 30 ± 12 pM
AdoHcy	poly(dI·dC−dI·dC)	AdoMet	NC/UC	nd[d]
AdoHcy	AdoMet	poly(dI·dC−dI·dC)	C	K_{is} 1.4 ± 0.2 μM

[a] AdoHcy, *S*-adenosylhomocysteine; AdoMet, *S*-adenosylmethionine; C, competitive; NC, noncompetitive; UC, uncompetitive inhibition. [b] K_{is} refers to the inhibition constant derived from a slope effect. K_{ii} refers to the inhibition constant derived from an intercept effect. [c] nd, not determined. The determination of an inhibition constant may be complicated by binding to a second nucleic acid binding site on the DCMTase. [d] nd, not determined. The inhibition constants are dependent on the fixed AdoMet concentration and inhibition is not overcome by saturating AdoMet concentrations. Instead, the inhibition profiles are noncompetitivelike at low AdoMet and uncompetitivelike at high AdoMet concentrations.

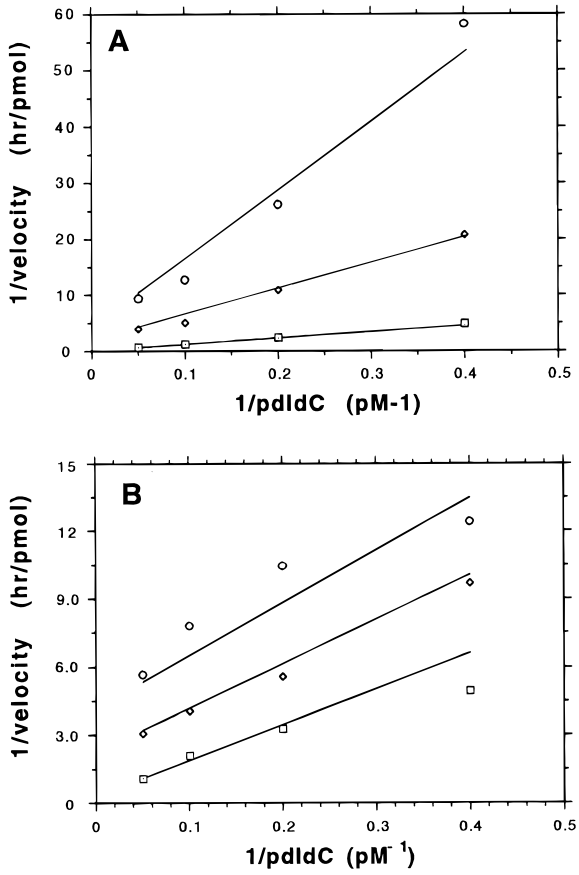

FIGURE 5: Double-reciprocal plot of AdoHcy product inhibition with varying poly(dI·dC−dI·dC) concentrations. Reactions contained 20 nM DCMTase in 100 mM Tris, pH 8.0, 10 mM EDTA, 10 mM DTT, and 200 μg/mL BSA. Incubations were at 37 °C for 60 min. The poly(dI·dC−dI·dC) concentrations were 2.5, 5.0, 10, and 20 pM. The AdoHcy concentrations were (□) 0; (◇) 15 μM; and (○) 30 μM. (Panel A) AdoMet held constant at 1.2 μM. (Panel B) AdoMet held constant at 8.0 μM. Experimental data are shown scattered around lines derived from a fit to eq 5 for noncompetitive inhibition.

order of substrate addition and product release should produce a series of four product inhibition plots that are all noncompetitive; therefore the pattern in Figure 4 is inconsistent with a random bi-bi mechanism. The competitive nature of AdoHcy with respect to AdoMet binding, K_{is} = 1.4 ± 0.2 μM, classically suggests that AdoMet and AdoHcy bind to the same form of the enzyme. Another explanation does not adhere to the simple model and predicts that, in an ordered bi-bi mechanism, if $K_{iq} \ll K_{mQ}$ then AdoMet binds after poly(dI·dC−dI·dC) and AdoHcy is the first product released. In considering this possibility, recall that in Figure 3 K_{ia} and K_{ib} were 10-fold less than the corresponding K_m

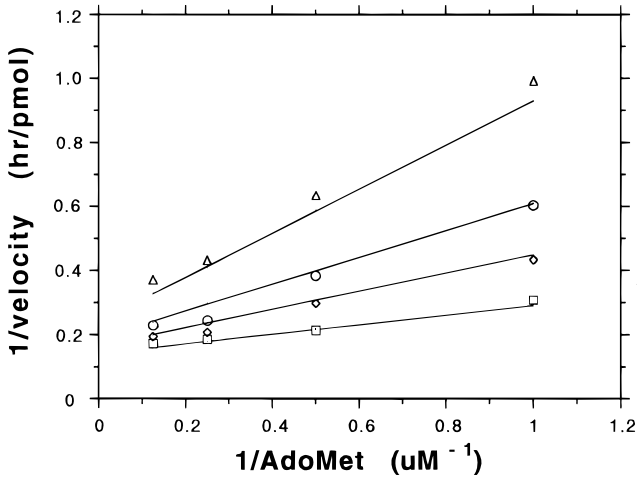

FIGURE 6: Double-reciprocal plot of poly(dI·d^{m}C−dI·d^{m}C) product inhibition with varying AdoMet concentrations. Reactions contained 20 nM DCMTase and 60 pM poly(dI·dC−dI·dC) in 100 mM Tris, pH 8.0, 10 mM EDTA, 10 mM DTT, and 200 μg/mL BSA. The AdoMet concentrations were 1.0, 2.0, 4.0, and 8.0 μM. The poly(dI·d^{m}C−dI·d^{m}C) concentrations were (□) 0; (◇) 5.0 pM; (○) 10 pM; and (△) 20 pM. Incubations were at 37 °C for 60 min. Experimental data are shown scattered around lines derived from a fit to eq 5 for noncompetitive inhibition.

values and this resulted in initial velocity patterns that were nearly parallel. Also, methylation at the C^5 position of pyrimidines is considered to be catalytically irreversible for a whole class of enzymes (*18*), suggesting again that K_{iq} may be significantly lower than K_{mQ} and that the competitive nature of AdoHcy to AdoMet with DCMTase may be indicative of an ordered bi-bi mechanism.

A distinctive inhibition profile was revealed when AdoHcy and poly(dI·dC−dI·dC) were varied. Two families of plots were obtained with AdoMet at different constant levels, 1.2 μM and 8.0 μM (Figure 5, panels A and B, respectively). Increasing the AdoMet concentration had the effect of changing the plots from a noncompetitive pattern at concentrations near K_m^{AdoMet} to an uncompetitive pattern at higher AdoMet concentrations. Note the decrease in scale of the *y*-axis in Figure 5B compared to Figure 5A and the lack of a significant change of the data collected at high poly(dI·dC−dI·dC) concentrations, the points closest to the *y*-axis. Graphical analysis of the data at high AdoMet concentrations appeared to fit slightly less well to an uncompetitive model, K_{ii} = 2.0 ± 0.6 μM, than to a noncompetitive model that produced the constants K_{is} = 63 ± 71 μM and K_{ii} = 2.5 ± 1.0 μM. The K_i^{AdoHcy} was independently determined in Figure 4 to be 1.4 μM. The slope and *y*-intercept replots from each AdoHcy versus poly-

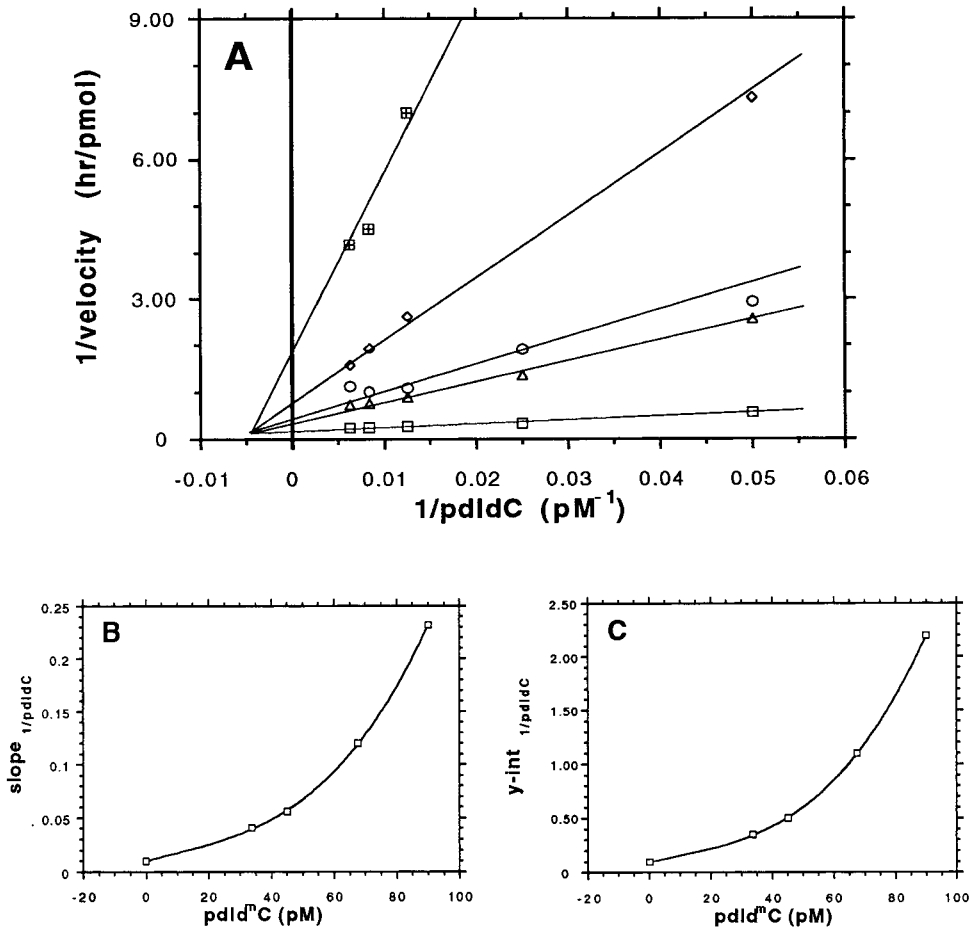

FIGURE 7: Double-reciprocal plot of poly(dI·d^{m}C−dI·d^{m}C) product inhibition with varying poly(dI·dC−dI·dC) concentrations. Reactions contained 20 nM DCMTase and 1.5 μM AdoMet in 100 mM Tris, pH 8.0, 10 mM EDTA, 10 mM DTT, and 200 μg/mL BSA. Incubations were at 37 °C for 60 min. The poly(dI·dC−dI·dC) concentrations were 20, 40, 80, 120, and 160 pM. The poly(dI·d^{m}C−dI·d^{m}C) concentrations were (□) 0; (△) 34 pM; (○) 45 pM; (◇) 68 pM, and (notched squares) 90 pM. Panel A shows the intersecting noncompetitive lines. Panel B is the slope replot, and panel C is the *y*-intercept replot obtained from the lines in panel A.

(dI·dC−dI·dC) series were all linear. Another study confirmed these results and showed a gradual effect of going from a noncompetitive to an uncompetitive model using three AdoMet concentrations: 1, 2.5, and 6.3 μM (data not shown). This analysis demonstrates that the slope contribution to AdoHcy inhibition is minimal at low AdoMet concentrations, inhibition cannot be overcome by high AdoMet concentrations, and AdoHcy binds to a different enzyme form than poly(dI·dC−dI·dC). This is strong evidence for an ordered bi-bi mechanism in which initial DNA binding is followed by AdoMet binding and that the following reaction step is irreversible:

$$\text{DCMTase}-\text{poly(dI·dC}-\text{dI·dC)} + \text{AdoMet} \rightarrow \text{DCMTase}-\text{poly(dI·dC}-\text{dI·dC)}-\text{AdoMet}$$

Also, the last product to leave the enzyme cannot be AdoHcy if poly(dI·dC−dI·dC) is the first substrate to bind DCMTase. Uncompetitive inhibition with AdoHcy and DNA was also observed with M.*Hha*I; it provided evidence that a M.*Hha*I−DNA−AdoHcy complex can form and ruled out a catalytically significant M.*Hha*I−AdoHcy complex (*20*).

Product Inhibition with Poly(dI·d^{m}C−dI·d^{m}C). Fully methylated poly(dI·d^{m}C−dI·d^{m}C) was prepared and used as a product inhibitor of the DCMTase reaction. Poly(dI·d^{m}C−dI·d^{m}C) was linear noncompetitive with AdoMet when poly-

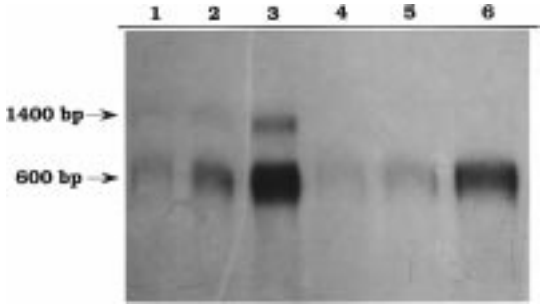

FIGURE 8: Molecular partitioning analysis. Lanes 1−3 are 1.5, 3, and 9 min time points from a reaction that preincubated DCMTase with 1400 base pair poly(dI·dC−dI·dC) and chased the initial complex with excess 600 base pair poly(dI·dC−dI·dC) and tritiated AdoMet. Lanes 4−6 are from a control reaction at the same times in which both DNA lengths were preincubated together with DCMTase, followed by addition of AdoMet to promote catalysis.

(dI·dC−dI·dC) was held constant (Figure 6). The estimated inhibition constants were $K_{is} = 5.3 \pm 2.1$ pM and $K_{ii} = 30 \pm 12$ pM. The noncompetitive pattern with AdoMet supports many different mechanisms, including one in which DNA binding occurs prior to AdoMet binding.

The double-reciprocal pattern for methylated DNA product versus DNA substrate would be expected to be competitive in a standard ordered bi-bi kinetic mechanism where DNA adds first and methylated DNA leaves last from the enzyme

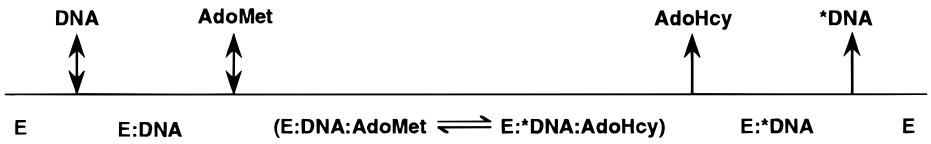

FIGURE 9: Proposed kinetic mechanism. DCMTase appears to progress through the catalytic cycle by the ordered bi-bi mechanism shown. Methylated DNA is denoted as *DNA.

surface. The double-reciprocal data obtained from five experiments appeared to be noncompetitive. However, upon fitting the data to the standard competitive and the noncompetitive models, graphical analysis showed that the fittings in both cases were not acceptable. This was also observed when AdoMet concentrations were held constant between 1.25 and 12.5 μM. The sensitivity to inhibition was notably abrupt, as poly(dI·d^{m}C−dI·d^{m}C) had little effect at 10 pM but completely inhibited the reaction at 100 pM. The results from one experiment are shown in Figure 7A with idealized lines intersecting left of the *y*-axis. Secondary slope and *y*-intercept replots (Figure 7B,C) were obtained, and both were parabolic concave upward. This explains the difficulty in fitting the simple model and is indicative of poly(dI·d^{m}C−dI·d^{m}C) binding at two points in the catalytic cycle. Furthermore, it is evidence that a DCMTase−DNA−DNA complex can be formed. Additional steady-state kinetic experiments also support the existence of an inhibitory DCMTase−DNA−DNA complex (manuscript in preparation).

Isotope Partitioning Analysis with AdoMet. Isotope partitioning analysis is a powerful strategy used to identify catalytically competent enzyme−substrate complexes (*39*, *40*). The DCMTase−AdoMet complex formed with 10 μM radiolabeled AdoMet was not competent for catalysis, because a chase including 400 pM poly(dI·dC−dI·dC) and 100 μM unlabeled AdoMet produced no detectable activity (data not shown). Substrate inhibition was not observed at high AdoMet concentrations. This is typical for an ordered bi-bi mechanism when studying the second substrate by isotope partitioning, because the DCMTase−AdoMet complex must dissociate before DCMTase can bind poly(dI·dC−dI·dC). Under these conditions, the DCMTase−poly(dI·dC−dI·dC) complex would then bind a diluted specific activity AdoMet and catalysis would not be detectable. Another potential explanation of the results predicts a rapid equilibrium binding of AdoMet as the first substrate in an ordered mechanism. However, this should have been obvious from varying each substrate as in Figure 3, because markedly different double-reciprocal patterns would have been resolved.

Molecular Partitioning Analysis. A novel assay was developed to test the competency of the initial DCMTase−poly(dI·dC−dI·dC) complex. This complex was formed with one DNA length, 1400 base pairs, and then challenged with an excess of smaller, 600 base pair DNA combined with labeled AdoMet. The initial DCMTase−poly(dI·dC−dI·dC) complex was observed to be competent for catalysis, because tritium was incorporated into the larger DNA (Figure 8). A control experiment allowed both DNA lengths to compete for DCMTase binding before AdoMet was added, because the smaller DNA was at a sufficiently high concentration the majority of the detectable label was incorporated into it.[2] This demonstrates quite clearly that DNA, under the conditions of our assays, can bind first in the steady-state mechanism and limits the assumptions made in our other experiments to the ordered bi-bi mechanism.

CONCLUSIONS

Under the conditions of our assays, the DCMTase purified from MEL cells has a kinetic order as follows: DNA binds DCMTase, then AdoMet binds and catalysis occurs, and then AdoHcy leaves the enzyme followed by methylated DNA (Figure 9). The proposed mechanism is similar to that described by Wu and Santi (*19*) for the bacterial DNA (cytosine-5-)-methyltransferase, M.*Hha*I. We suggest that the intersecting double-reciprocal plots for a rapid equilibrium ordered bi-bi mechanism observed with M.*Hha*I and our observation of double-reciprocal plots that intersect far from the *y*-axis with the murine DCMTase may be reconciled by differences in the lifetimes and partitioning of catalytic intermediates. Candidate differences include assembly of the E−DNA−AdoMet intermediate complex where the target cytosine is stabilized within the enzyme, the covalent E−DNA−AdoMet complex, or subsequent steps involving methyl transfer or β-elimination. The mammalian DCMTase is approximately 3 times larger than the bacterial enzymes and contains a large amino-terminal domain, the regulation of which may directly influence catalysis.

The single-displacement mechanism postulated for the M.*Hha*I places stereochemical and kinetic constraints on the reaction. Methyl transfer from AdoMet to cytosine position C^5 proceeds with an inversion of stereochemistry at the transferred methyl group (*18*), as predicted for a bimolecular reaction in which the methyl group transfers directly from AdoMet to the cytosine. This is characteristic of sequential mechanisms and the rapid equilibrium ordered bi-bi mechanism used by M.*Hha*I. Although the stereochemistry is not known for the murine enzyme, the sequential ordered mechanism that it apparently uses is similar to that used by the bacterial enzyme.

Quantitative enzymological studies reveal a great deal about how enzymes function and can yield novel insights into biological phenomena. The evidence that poly(dI·d^{m}C−dI·d^{m}C) can bind to two enzyme forms in the catalytic cycle is intriguing, and although processivity has not been addressed in our studies, the kinetic mechanism proposed is that expected for a processive enzyme. Our laboratory is now positioned to study the biochemistry of the different isoforms of the DCMTase that may exist in mammals and how cellular factors or DNA conformations modulate DCMTase function.

[2] A similar result was obtained by J.F. using M.*Hha*I (Lindstrom, Flynn, and Reich, manuscript in preparation).

ACKNOWLEDGMENT

We thank Dr. W. W. Cleland, Dr. Stanley M. Parsons, and Dr. Norbert Brunhuber for many helpful discussions throughout the course of this work. We also thank Dr. W. W. Cleland, Dr. W. Brent Derry, and Dr. John Lew for reviewing the manuscript and making critical comments.

REFERENCES

1. Boyes, J., and Bird, A. P. (1991) *Cell 64*, 1123−1134.
2. Razin, A., and Riggs, A. D. (1980) *Science 210*, 604−609.
3. Kafri, T., Ariel, M., Brandeis, M., Shemer, R., Urven, L., McCarrey, J., Cedar, H., and Razin, A. (1992) *Genes Dev. 6*, 705−714.
4. Jost, J. P., and Saluz, H. P. (1993) *DNA Methylation: Molecular Biology and Biological Significance*, Birkhauser Verlag, Basel, Switzerland.
5. Li, E., Bestor, T. H., and Jaenisch, R. (1992) *Cell 69*, 915−926.
6. Szyf, M. (1996) *Pharmacol. Ther. 70*, 1−37.
7. Jones, P. A. (1996) *Cancer Res. 56*, 2463−2467.
8. Bestor, T., Laudano, A., Mattaliano, R., and Ingram, V. (1988) *J. Mol. Biol. 203*, 971−983.
9. Yen, R. C., Vertino, P. M., Nelkin, B. D., Yu, J. J., El-Deiry, W., Cumaraswamy, A., Lennon, G. G., Trask, B. J., Celano, P., and Baylin, S. B. (1992) *Nucleic Acids Res. 20*, 2287−2291.
10. Tajima, S., Tsuda, H., Wakabayashi, N., Asano, A., Mizuno, S., and Nishimori, K. (1995) *J. Biochem. (Tokyo) 117*, 1050−1057.
11. Kimura, H., Ishihara, G., and Tajima, S. (1996) *J. Biochem. (Tokyo) 120*, 1182−1189.
12. Aniello, F., Locascio, A., Fucci, L., Geraci, G., and Branno, M. (1996) *Gene 178*, 57−61.
13. Posfai, J., Bhagwat, A. S., Posfai, G., and Roberts, R. J. (1989) *Nucleic Acids Res. 17*, 2421−2435.
14. Leonhardt, H., Page, A. W., Weier, H., and Bestor, T. H. (1992) *Cell 71*, 865−873.
15. Bestor, T. H. (1992) *EMBO J. 11*, 2611−2617.
16. Chuang, L. S., Ng, H., Chia, J., and Li, B. F. L. (1996) *J. Mol. Biol. 257*, 935−948.
17. Glickman, J. F., Pavlovich, J. G., and Reich, N. O. (1997) *J. Biol. Chem. 272*, 17851−17857.
18. Ivanetich, K. M., and Santi, D. V. (1992) *Prog. Nucleic Acid Res. Mol. Biol. 42*, 127−156.
19. Wu, J. C., and Santi, D. V. (1987) *J. Biol. Chem. 262*, 4778−4786.
20. Klimasauskas, S., Kumar, S., Roberts, R. J., and Cheng, X. (1994) *Cell 76*, 357−369.
21. Osterman, D. G., DePhillis, G. D., Wu, J. C., Matsuda, A., and Santi, D. V. (1988) *Biochemistry 27*, 5204−5210.
22. Laird, P. W., Jackson-Grusby, L., Fazell, A., Dickinson, S. L., Jung, W. E., Li, E., Weinberg, R. A., and Jaenisch, R. (1995) *Cell 81*, 197−205.
23. Belinsky, S. A., Nikula, K. J., Baylin, S. B., and Issa, J. J. (1996) *Proc. Natl. Acad. Sci. U.S.A. 93*, 4045−4050.
24. Chuang, L. S., Ian, H. I., Koh, T. W., Ng, H. H., Xu, G., and Li, B. F. (1997) *Science 277*, 1996−2000.
25. Zhang, X. Y., and Verdine, G. L. (1996) *FEBS Lett. 392*, 179−183.
26. Lei, H., Oh, S. P., Okano, M., Juttermann, R., Goss, K. A., Jaenisch, R., and Li, E. (1996) *Development 122*, 3195−3205.
27. Pradhan. S., Talbot, D., Sha, M., Benner, J., Hornstra, L., Li, E., Jaenisch, R., and Roberts, R. J. (1997) *Nucleic Acids Res. 25*, 4666−4673.
28. Xu, G., Flynn, J., Glickman, J. F., and Reich, N. O. (1995) *Biochem. Biophys. Res. Commun. 207*, 544−551.
29. Flynn, J., Glickman, J. F., and Reich, N. O. (1996) *Biochemistry 35*, 7308−7315.
30. Flynn, J., Azzam, R., and Reich, N. O. (1998) *J. Mol. Biol. 279*, 101−116.
31. Pedrali-Noy, G., and Weissbach, A., (1986) *J. Biol. Chem. 261*, 1, 7600−77602.
32. Cleland, W. W. (1963) *Biochim. Biophys. Acta 67*, 104−137.
33. Cleland, W. W. (1963) *Biochim. Biophys. Acta 67*, 173−187.
34. Cleland, W. W. (1979) *Methods Enzymol. 63*, 103−138.
35. Surby, M., and Reich, N. O. (1996) *Biochemistry 35*, 2201−2008.
36. Surby, M., and Reich, N. O. (1996) *Biochemistry 35*, 2209−2217.
37. Alberty, R. A. (1958) *J. Am. Chem. Soc. 80*, 1777.
38. Rudolph, F. B. (1979) *Methods Enzymol. 63*, 411−436.
39. Rose, I. A. (1980) *Methods Enzymol. 64*, 47−59.
40. Reich, N. O., and Mashhoon, N. (1991) *Biochemistry 30*, 2933−2939.

BI9810609